Design of Low-Loss Tapered Waveguides Using the Telescope Structure Compensation

Chun-Wen Chang, Mount-Learn Wu, and Wen-Feng Hsieh

***Abstract*—A low-loss tapered waveguide is achieved by the telescope structure compensation. The configuration of this design is similar to the Galilean telescope based on the bulk geometrical optics. We numerically calculate the transmission efficiency in the use of the beam propagation method (BPM) and the finite-difference time-domain method. The BPM simulation results reveal that the normalized transmission efficiency is more than 95%, even if the tapered angle is as large as 10°.**

***Index Terms*—Tapered waveguides, telescope structure compensation.**

I. Introduction

HIGHLY EFFICIENT optical-coupling with a large misalignment tolerance between two photonic guided-wave devices with different cross-sectional dimensions is important in various electrooptical applications. The tapered waveguide is one of the popular means of converting optical mode sizes [1] to connect different electrooptical devices. However, the tapered waveguide suffers serious radiation loss due to the mode mismatching as its tapered angle increases. To reduce the excessive loss, the dimensional variation along the propagation direction of a tapered waveguide is limited, so that it is difficult to design a compact structure with shorter taper length. Therefore, how to design a practical tapered waveguide with characteristics of wide angle but low loss is an important topic.

A number of methods [1], have been proposed to increase the coupling efficiency of the tapered waveguide.

A novel approach to design a high-efficiency and compact-size lateral tapered waveguide is proposed in this letter. As presented in Fig. 1, the Galilean telescope compensator provides a low-loss beam-shaping method that converts a broad plan-wave beam into a small one and, thus, it is easily coupled to the following guided-wave structure. This high conversion ratio structure can combine the multilayer tapered waveguide structure [2] to efficiently couple a multimode fiber into a single-mode fiber. Computer simulation using the beam propagation method (BPM) is implemented to demonstrate the mode-conversion performance of the proposed structures. Furthermore, the fabrication issues, including the dimensional deviations and the surface roughness of the lenses, are also investigated to evaluate the practicability. By using the simulation of finite-difference time-domain (FDTD) method, the curved-wavefront phenomenon is revealed in the practical taper region.

Manuscript received December 17, 2002; revised June 19, 2003. This work was supported by the National Science Council, Taiwan, under Grant NSC-912 112M009040.

C.-W. Chang and W.-F. Hsieh are with the Institute of Electro-Optical Engineering, National Chiao Tung University, Hsinchu, Taiwan 30050, R.O.C. (e-mail: wfhsieh@mail.nctu.edu.tw).

M.-L. Wu is with the Neostones Microfabrication Company, Ltd., Hsinchu, Taiwan 300, R.O.C.

Digital Object Identifier 10.1109/LPT.2003.818253

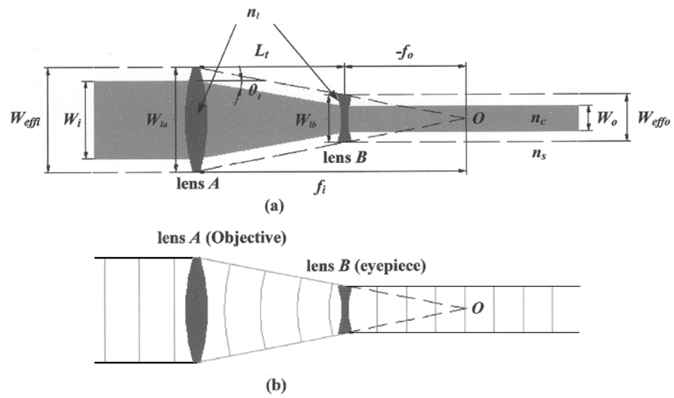

Fig. 1. (a) Telescope structure compensation lenses in the tapered waveguide and (b) the Galilean telescope system.

II. Design Rule

The proposed tapered waveguide is shown in Fig. 1(a). As can be seen in this figure, a compensation lens set based on the configuration of Galilean telescope is disposed in the tapered region of the proposed waveguide. Lens A with a positive focal length f_i and lens B with a negative focal length $-f_o$ are placed in the input and output ends of the tapered region, respectively. Point O is the common focus of both lenses.

As shown in Fig. 1(b), the eigenmode with planar wavefronts in the input straight end of the tapered waveguide is collected by lens A and then converges toward the focus O. Consequently, the mode size of lightwave is converted continuously in the tapered region and the planar wavefronts become curved ones. After passing through lens B, the converged wave is diverged into a planar one with a decreased mode size and propagates smoothly in the output end of tapered waveguide.

As illustrated in Fig. 1(a), W_{la} and W_{lb} are apertures of lens A and lens B, respectively. L_t represents the length of the tapered region and θ_t is the tapered angle. Geometrically, L_t can be expressed as

$$L_t = \left(\frac{W_i - W_o}{2\tan\theta_t}\right) \tag{1}$$

where W_i and W_o represent the input and output waveguide width, respectively.

As presented in Fig. 1(a), the effective waveguide width is used as the aperture of the corresponding lens and the focal length of lens A can be obtained from

$$\sin(\theta_t) = \frac{W_{\text{eff}\,i}/2}{\sqrt{(W_{\text{eff}\,i}/2)^2 + f_i^2}}. \tag{2}$$

Consequently, from (2), the focal length f_i of lens A can be determined as the geometry of waveguide is given. Due to the coincidence of the focal points of lens A and lens B, we have

$$(-f_o) = f_i - L_t. \tag{3}$$

Thus, the focal length $-f_o$ of lens B can be also obtained.

In order to determine the materials and radii of curvature adopted for the compensation lens set, the Lensmaker's formula of the thin lens approximation is used and described as below. If a lens with a given refractive index n_l and given radii of curvature R_1 and R_2 are used in an ambient medium of refractive index n_m, its focal length f can be formulated as

$$\frac{n_m}{f} = (n_l - n_m)\left(\frac{1}{R_1} + \frac{1}{R_2}\right). \tag{4}$$

In the analysis, the refractive index of the ambient material can be approximated as the effective refractive index n_{eff} of the waveguide, which is defined as the ratio of the propagation constant of the waveguide to the wavenumber in vacuum. As the focal length and lens material are chosen, the radii of curvature of lens A and lens B are determined.

III. Numarical Results and Discussion

To examine the performance of the telescope structure compensation design, an example of tapered waveguide with high conversion ratio W_i/W_o of five is analyzed. As can be seen in Fig. 1(a), the width of the input end of the tapered waveguide W_i is assumed to be 45 μm and that of the output end W_o is equal to 9 μm. The refractive indexes of $n_s = 1.5$ and $n_c = 1.504$ are used for the cladding layer and core material. The exciting wavelength of a fundamental transverse electric mode in this analysis is 1.5 μm. According to the above information, the effective refractive indexes $n_{\text{eff}\,i}$ and $n_{\text{eff}\,o}$ for both input and output straight ends can be calculated as 1.503 923 and 1.502 983, respectively.

Various kinds of materials and corresponding curvatures can be chosen to bend the phase front before and after the tapered region. In the analysis, Si_3N_4 $(n = 2.0)$ is adopted to be the compensation material of both lenses. Furthermore, the effective refractive indexes $n_{\text{eff}\,i}$ and $n_{\text{eff}\,o}$ of both input and output straight ends are employed as the parameter of n_m in (4) for lens A and lens B, respectively. In the following simulations, in order to precisely apply the BPM to the proposed structures, the transparent boundary condition is adopted to avoid the reflections occurring in the boundaries of the computational domain. And the high-order approximation is also employed to eliminate the inaccuracy due to wide angle and large differences of refractive indexes. Note that the tapered angles from 1° to 20° are analyzed in the proposed tapered waveguides, and the corresponding radii of curvatures of lens A and B used in the proposed compensated structures are shown in Fig. 2. As revealed by this figure, the larger the tapered angle, the smaller the radius will be needed and the smallest radii of curvatures occurring at the case of $\theta_t = 20°$ are 44.8 and 12.8 μm for lens A and lens B, respectively.

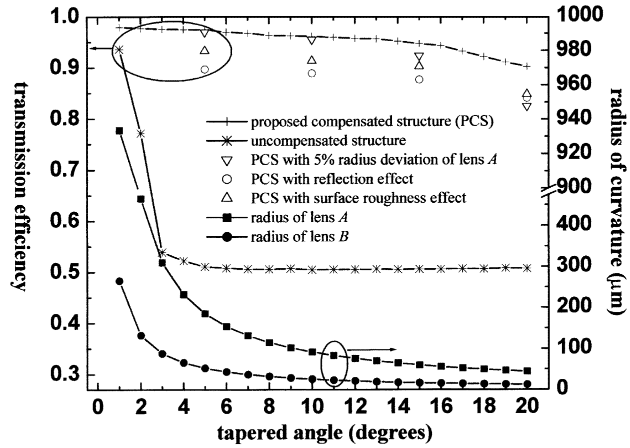

Fig. 2. Variation in the radii of the lenses and the normalized transmission power efficiency versus the tapered angle.

The normalized transmission efficiency η of the tapered structure, which is defined as the ratio of the output power and the input power versus the tapered angle are also shown in Fig. 2. The propagation loss of the uncompensated tapered waveguide (the curve labeled with $*$) is about 50% when the tapered angle is larger than 5°. However, the transmission efficiency of the proposed structure (labeled with $+$) is as high as 88%, even if the tapered angel is 20°. Since the lens is using the higher reflective indexes, the propagation loss owing to the reflection must be taken into consideration. However, the single-directional BPM is not suitable to simulate the reflection induced in the boundaries between the waveguides and the lenses. The FDTD method is employed to calculate the transmission efficiency of proposed structures with reflection in Fig. 2. It shows only 6%–7% additional reflection losses are introduced as the tapered angle θ_t varies from 5° to 20°. The results consistent with those obtained from the Fresnel's equations are independent of the tapered angles.

However, the tapered waveguide is practically a three-dimensional (3-D) structure rather than a two-dimensional (2-D) one. To compare the 3-D calculation with the 2-D one, we used the above-mentioned parameters with $\theta_t = 10°$, and assumed the slab thickness $h_s = 6.4$ μm, and let the thickness of the compensation lens be larger than the height of the effective mode cross section to avoid the radiation losses in the vertical direction. We found that the transverse field distributions are well confined within the input waveguide, the tapered region, and the output waveguide, respectively. The transmission efficiency is 91% for the 3-D result and is 95% for 2-D one. As a result, the 2-D calculation in this analysis would not deviate significantly from the 3-D one and can provide a good demonstration of the proposed structure.

To demonstrate the practicability of the proposed structures, two major fabrication considerations regarding the dimension deviation and the surface roughness of the introduced lenses are also studied. Fig. 2 shows the transmission efficiencies of the

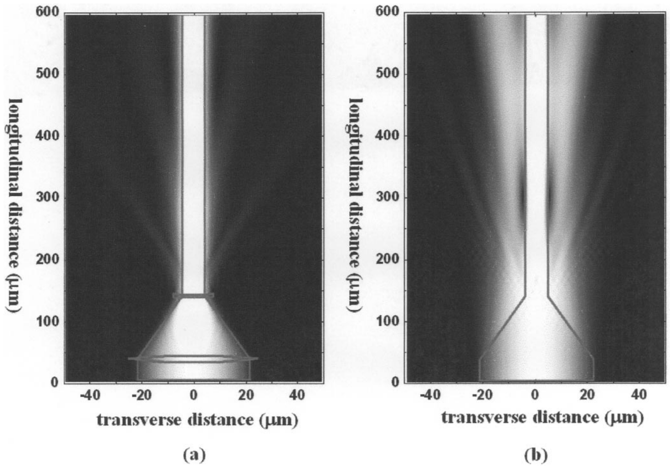

Fig. 3. Field distribution of the (a) compensated and (b) uncompensated tapered waveguides ($W_i = 45\ \mu$m, $W_o = 9\ \mu$m, and $\theta_t = 10°$).

proposed tapered waveguides considering the radius deviation. Assuming +5% radius deviation (corresponding to $+2.24$-μm dimension deviation) of lens A, we found the transmission efficiencies of the proposed tapered waveguides at the most detrimental situation occur for $\theta_t = 20°$ has the maximum 7.7% propagation loss. Moreover, in the practical fabrication, e.g., using the reactive ion etching, the surface roughness less than 0.2 μm are achievable. In this analysis, we enlarged the grid size from 0.05 (corresponding to $1/20$ wavelength) to 0.2 μm to simulate the surface roughness of 0.2 μm for the lenses. Also shown in Fig. 2, the surface roughness of 0.2 μm induces acceptable excessive losses of 4%–5% as θ_t varies from 5° to 20°.

Fig. 3 shows the field intensity distribution of the tapered waveguide with and without the compensation lens set. The tapered angle in this case is 10°. It can be found that the power radiates out continuously in the tapered region due to the mode mismatching. In comparison with the previous case, the radiation pattern of the compensated one becomes more convergent and the normalized transmitted power efficiency of that is as high as 95%. In addition to the high-transmitted power efficiency, the converted mode becomes stable rapidly after leaving the tapered region; therefore, the size of the tapered waveguide will become more and more compact.

Fig. 4 illustrates the relation between the transmitted power efficiency and the conversion ratio W_i/W_o for compensated and uncompensated structures when the tapered angle is 10°. As can be seen, the transmission efficiency of the proposed structure is stable under the variation of W_i/W_o; however, the efficiency decreases rapidly for uncompensated structure when the conversion ratio grows up.

In order to obtain an insight into the wavefront transition, the FDTD method is employed to calculate the electromagnetic field distribution in the proposed structure. For easier observation, an example of small conversion ratio W_i/W_o of three is simulated. The width of input waveguide is 27 μm and that of the output one is 9 μm. Fig. 5 displays the calculation results of the electric field distribution. As shown in this figure, owing to the telescope structure energy transportation system, the phase front is curved toward the focus and flattened again while leaving the tapered region. Thus, the eigenmode of the input waveguide will become stable rapidly and transfer smoothly to the output waveguide.

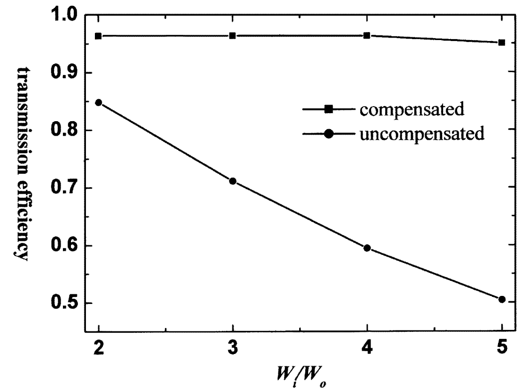

Fig. 4. Transmitted power efficiency versus the conversion ratio W_i/W_o of the compensated and the uncompensated tapered waveguides

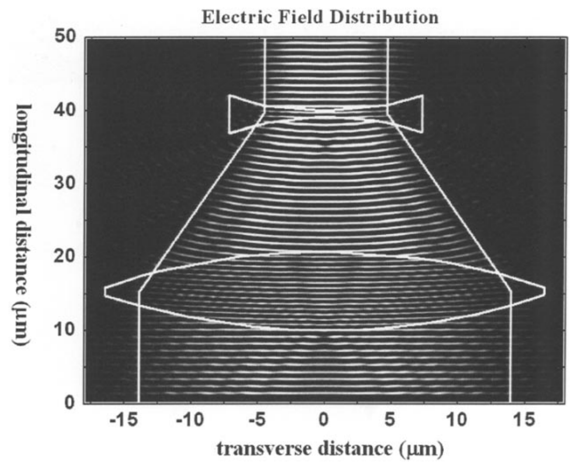

Fig. 5. Electric field distribution calculated by the FDTD method ($W_i = 27\ \mu$m, $W_o = 9\ \mu$m, and $\theta_t = 20°$).

IV. Conclusion

In this letter, a novel lateral tapered waveguide with the telescope structure compensation region has been proposed. Owing to the compensation lens set, the wavefront of the light wave in the waveguide can be modulated, and thus, the eigenmode of the input waveguide can be transferred smoothly. Furthermore, the BPM calculation results reveal that the proposed structures have good performances in the transmission efficiency and the fabrication tolerances. Therefore, the telescope structure compensation can be implemented in the real application of highly compact tapered waveguides.

References

[1] O. Mitomi, K. Kasaya, and H. Miyazawa, "Design of a single-mode tapered waveguide for low-loss chip-to-fiber coupling," *IEEE J. Quantum Electron.*, vol. 30, pp. 1787–1793, Aug. 1994.

[2] R. S. Fan and R. B. Hooker, "Tapered polymer single-mode waveguides for mode transformation," *J. Lightwave Technol.*, vol. 17, pp. 466–474, Mar. 1999.